International Journal of Heat and Mass Transfer 177 (2021) 121465

Contents lists available at ScienceDirect

International Journal of Heat and Mass Transfer

journal homepage: www.elsevier.com/locate/hmt

Multilayer one-dimensional Convection-Diffusion-Reaction (CDR) problem: Analytical solution and imaginary eigenvalue analysis

Ankur Jain[a,*], Long Zhou[b,1], Mohammad Parhizi[a,1]

[a] Mechanical and Aerospace Engineering Department, University of Texas at Arlington, Arlington, TX, USA
[b] School of Mechanical and Power Engineering, Henan Polytechnic University, Jiaozuo, Henan, China

ARTICLE INFO

Article history:
Received 4 March 2021
Revised 12 April 2021
Accepted 6 May 2021

Keywords:
Convection-Diffusion-Reaction (CDR) equation
Multilayer body
Eigenvalues
Imaginary numbers

ABSTRACT

This paper presents a theoretical analysis of a one-dimensional multilayer heat transfer problem with diffusion, advection and linear temperature-dependent heat generation occurring in each layer. A general solution of the problem is derived. Orthogonality of eigenfunctions is proved, and an explicit expression for the eigenequation is derived. The special case of a two-layer body is discussed. It is shown that, under specific conditions, this problem admits two types of imaginary eigenvalues, one of which is related to divergence of temperature at large times, corresponding to the thermal runaway phenomenon in batteries. The impact of various problem parameters related to diffusion, advection and heat generation on the appearance of imaginary eigenvalues is discussed. Specifically, due to the directional nature of fluid flow, advection in each layer of a two-layer body has opposing impact on the occurrence of imaginary eigenvalues. It is also shown that a balance between heat generation, diffusion and advection determines whether an imaginary eigenvalue is encountered, and consequently, whether thermal runaway occurs. Results presented here expand the theoretical understanding of multilayer heat transfer, and may also contribute towards improved thermal design of multilayer engineering systems such as flow batteries.

1. Introduction

Heat and mass transport in a multilayer body [1] has been investigated in several past papers for a variety of engineering and biomedical applications. For example, mass transfer in a multilayer structure has been used for modeling drug delivery in drug eluting stents [2]. Thermal transport in biological tissue has been modeled using multilayer Pennes equation that contains a temperature-dependent perfusion term [3]. Heat transfer in multilayered bodies is also relevant for several traditional engineering fields, such as manufacturing [4], atmospheric re-entry [5], extended surfaces [6], microelectronics cooling [7] and nuclear power generation [8].

Key physical processes that occur in multilayer heat and mass transfer problems include diffusion, advection due to fluid flow and generation/consumption. The rate of generation or consumption of heat/mass is often proportional to the local temperature/concentration. For example, a chemical reaction with first-order kinetics consumes/generates species at a rate proportional to the local concentration of the reactant. Heat generated by such a chemical reaction is also often approximated as linearly temperature-dependent [9,10], even though, strictly speaking, the dependence is exponential in nature, as modeled by Arrhenius kinetics [11]. In addition, the perfusion term in the Pennes bioheat transfer equation [12] may also be interpreted as an energy consumption term proportional to the local temperature. Finally, the fin equation used for analysis of multilayer segmented fin may also be interpreted to contain a negative heat generation term that is proportional to the local temperature [6].

A transient energy conservation equation representing a balance between diffusion, advection and generation in each layer of an M-layer one-dimensional body may be written as [2]

$$\frac{\partial T_m}{\partial t} = \alpha_m \frac{\partial^2 T_m}{\partial x^2} - U_m \frac{\partial T_m}{\partial x} + \beta_m T_m (m = 1, 2, 3 \ldots M) \tag{1}$$

where T_m is the temperature field relative to ambient in the m^{th} layer.

A similar equation can be written for the concentration field in a mass transfer problem. This equation is often referred to as the Convection-Diffusion-Reaction (CDR) equation [13,14], and has been heavily researched for both heat and mass transfer problems. This problem is distinct from the pure-diffusion multilayer problem analyzed in textbooks [1] due to the appearance of convection and reaction terms. The eigenvalues and orthogonality relationships for CDR problems are likely to be very dif-

* Corresponding author at: 500W First St, Rm 211, Arlington, TX, USA 76019
E-mail address: jaina@uta.edu (A. Jain).
[1] Equal contributors

https://doi.org/10.1016/j.ijheatmasstransfer.2021.121465
0017-9310/

Nomenclature

Bi	Biot number
c	coefficient
h	convective heat transfer coefficient ($Wm^{-2}K^{-1}$)
i	unit imaginary number, $i = \sqrt{-1}$
k	thermal conductivity ($Wm^{-1}K^{-1}$)
$\bar{k}$	non-dimensional thermal conductivity
M	number of layers
N	eigenvalue norm
Pe	Non-dimensional velocity
T	temperature rise above ambient (K)
U	velocity (ms^{-1})
x	spatial coordinate (m)
t	time (s)
α	diffusivity (m^2s^{-1})
$\bar{\alpha}$	non-dimensional diffusivity
β	generation/consumption coefficient (s^{-1})
$\bar{\beta}$	non-dimensional generation/consumption coefficient
γ	non-dimensional interface location
τ	non-dimensional time
θ	non-dimensional temperature
ω	non-dimensional eigenvalue
ξ	non-dimensional spatial coordinate
λ	non-dimensional eigenvalue

Subscripts

A,B	left and right ends, respectively, of the multilayer body
m	layer number
0	initial value

ferent from the ones for pure-diffusion multilayer problems discussed in textbooks. Analytical approaches for solving CDR problems include an eigenfunction-based series solution [1] that uses quasi-orthogonality of the eigenfunctions [15,16] and an appropriate transformation to account for the effect of advection and generation [17]. The nature of orthogonality of eigenfunctions depends strongly on the presence of advection and the specific nature of boundary conditions. A number of unique interface conditions between layers in mass transfer problems involving porous media have been presented [17]. Analytical solutions for a variety of convection-diffusion problems – a subset of the CDR problem – have also been presented [18,19].

Several previous studies have developed analytical, semi-analytical, and numerical solutions of problems governed by the CDR equation. For example, the separation of variables technique was used to derive an exact solution for mass diffusion through a two-layer porous media with pure diffusion in one layer and all three phenomena in the other one [17,20]. A similar technique was also used to solve a more general CDR problem in multilayer porous media [21]. Laplace transformation technique has been used to derive an analytical solution to a two-layer CDR problem for drug-eluting stent problems [22]. A semi-analytical model for solute transport in multilayer porous media using Laplace transformation has been presented [23]. Several studies have used numerical techniques such as Additive Runge–Kutta [14,24], Positivity-Preserving Variational (PPV) [25], and Boundary Element Method [26] to solve more complicated CDR problems involving higher dimensions, non-linear terms, and variable coefficients. Various types of convection-diffusion problems have been solved using the method of eigenfunction expansions [27], integral transform [28,29] and separation of variables [30].

A limited amount of past work suggests that imaginary eigenvalues may be encountered in multilayer heat/mass transport problems. The first class of such problems pertains to 2D [31,32,33] and 3D [34] multilayer diffusion problems. In such problems, imaginary eigenvalues appear in the thickness direction due to real eigenvalues in the orthogonal direction(s). The second class of problems with imaginary eigenvalues involves multiple transport and generation processes in each layer, even for a one-dimensional body. For example, it has been suggested that eigenvalues may become imaginary in a one-dimensional two-layer mass transfer problem with diffusion in one layer and a combination of diffusion, advection and generation in the second layer [17]. However, a detailed analysis of conditions in which such eigenvalues may appear and their physical interpretation is missing. In recent work, an analysis of imaginary eigenvalues appearing in multilayer diffusion-reaction problems [35] has been presented. While this work derived the conditions in which imaginary eigenvalues appear and discussed their physical interpretation, the impact of advection was not considered. A complete analysis including the effect of advection is needed for modeling systems where advection plays a key role.

Imaginary eigenvalues are not merely a theoretical curiosity because certain imaginary eigenvalues in one-dimensional multilayer problems are directly related to the phenomenon of thermal runaway [35], in which, the temperature field diverges at large times. Prediction of imaginary eigenvalues and thermal runaway is of much practical importance for the safety of engineering systems such as Li-ion cells and battery packs. Specifically, in a flow battery [36] where the electrolyte is circulated, diffusion, advection and heat generation due to electrochemical reactions all occur simultaneously. In order to ensure the safety and reliability of such systems, it is important to develop a robust theoretical understanding of the regimes in which an imbalance between diffusion, advection and generation may lead to imaginary eigenvalues, and therefore, thermal runaway. In addition, understanding imaginary eigenvalues is important because a series solution must include all eigenvalues, whether real or imaginary, and standard methods for computing eigenvalues may miss an imaginary eigenvalue.

This paper presents the solution of a multilayer one-dimensional CDR heat transfer problem and specifically investigates the conditions that result in imaginary eigenvalues in such a problem. A solution is first presented for a general multilayer problem, followed by discussion of a special case of a two-layer body. A physical interpretation of imaginary eigenvalues in terms of a balance between conduction, advection and generation is presented. Within the context of a two-layer body, conditions for appearance of two types of imaginary eigenvalues are discussed. It is shown that the first type of imaginary eigenvalues results in thermal runaway in the body. The analysis of conditions that lead to imaginary eigenvalues may help in better design of multilayer systems in practical problems such as a flow battery.

This paper is organized as follows: the next section presents the general, M-layer problem and its solution, including derivation of the eigenequation and the orthogonality of eigenfunctions. The specific case of a two-layer body is discussed in Section 3. Section 4 then derives a mathematical requirement for the occurrence of imaginary eigenvalues. Several aspects of the conditions in which imaginary eigenvalues may appear – and their relationships with parameters associated with diffusion, advection and generation – are discussed in Section 5.

2. General M-layer body

Consider a one-dimensional M-layer body such as shown in Fig. 1(a). Heat is generated within each layer at a rate proportional to the local temperature. Heat transfer occurs within this

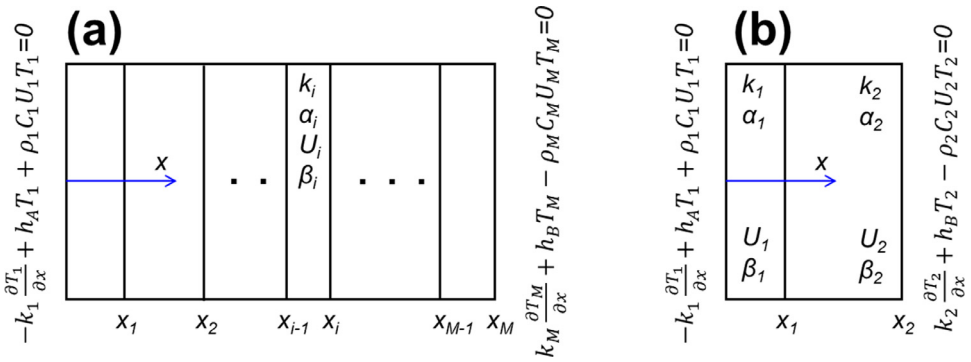

Fig. 1. Schematics of the (a) *M*-layer and (b) two-layer one-dimensional geometries with diffusion, one-dimensional flow and linear, temperature-dependent heat generation in each layer. A general convective boundary condition is also assumed at both ends.

body due to diffusion and due to advection driven by an imposed one-dimensional fluid flow in each layer from left to right. Each layer has distinct thermal properties, flow velocity and rate of heat generation. General convective boundary conditions are assumed on the left and right boundaries, respectively. The goal of the analysis is to predict the transient temperature distribution within the multilayer body. Note that based on the analogy between heat and mass transfer, the analysis presented below can be readily applied to a mass transfer problem, where concentration distribution in a multilayer body is governed by diffusion, advection and species generation/consumption at a rate proportional to the local concentration. Appropriate adjustments may need to be made to account for changes in boundary and interface conditions, for example due to porous flow specific to the mass transfer problem [17].

The governing equation based on energy conservation for this problem was presented as Eq. (1) in the previous section. In this equation, often referred to as the Convection-Diffusion-Reaction (CDR) equation, the first two terms on the right hand side represent heat transfer due to diffusion and advection, respectively, and the third term represents heat generation/consumption that is proportional to the local temperature. α_m and U_m are the thermal diffusivity and flow speed, respectively, in the m^{th} layer. Note that each layer may have distinct speeds without violating mass conservation, since the fluid density in each layer may be different. Finally, β_m is the source coefficient that relates the rate of heat generation to the local temperature. All properties are assumed to be independent of temperature.

General boundary conditions associated with Eq. (1) are

$$-k_1\frac{\partial T_1}{\partial x}+h_AT_1+\rho_1C_1U_1T_1=0 \ at \ x=0 \tag{2}$$

and

$$k_M\frac{\partial T_M}{\partial x}+h_BT_M-\rho_MC_MU_MT_M=0 \ at \ x=x_M \tag{3}$$

These boundary conditions represent a balance between convective heat transfer between the body and the ambient, and diffusion and advection into and out of the body. Note that while advection conveys energy from the ambient into the first layer, it removes energy from the M^{th} layer into the ambient.

In addition, temperature continuity and heat flux conservation at the interfaces in the body result in the following conditions for m = 1,2..*M*-1:

$$T_m=T_{m+1} \ at \ x=x_m \tag{4}$$

and

$$-k_m\frac{\partial T_m}{\partial x}+\rho_mC_mU_mT_m=-k_{m+1}\frac{\partial T_{m+1}}{\partial x}+\rho_{m+1}C_{m+1}U_{m+1}T_{m+1} \ at \ x=x_m \tag{5}$$

Finally, each layer is assumed to be at a given initial temperature

$$T_m=T_{m,0}(x) \ at \ t=0 \ (m=1,2\ldots M) \tag{6}$$

The set of Eqs. (1)-(6) are non-dimensionalized to ensure generality of the results. The following variables are introduced: $\theta_m=\frac{T_m}{T_{ref}}$, $\xi=\frac{x}{x_M}$, $\tau=\frac{\alpha_M t}{x_M^2}$, $\gamma_m=\frac{x_m}{x_M}$, $\bar{k}_m=\frac{k_m}{k_M}$, $\bar{\alpha}_m=\frac{\alpha_m}{\alpha_M}$, $Pe_m=\frac{U_m x_M}{\alpha_M}$, $\bar{\beta}_m=\frac{\beta_m x_M^2}{\alpha_M}$, $\theta_{m,0}=\frac{T_{m,0}}{T_{ref}}$, $Bi_A=\frac{h_A x_M}{k_M}$, $Bi_B=\frac{h_B x_M}{k_M}$. Here, T_{ref} is an arbitrary reference temperature.

Based on these parameters, the non-dimensional set of CDR equations for the multilayer body are

$$\frac{\partial\theta_m}{\partial\tau}=\bar{\alpha}_m\frac{\partial^2\theta_m}{\partial\xi^2}-Pe_m\frac{\partial\theta_m}{\partial\xi}+\bar{\beta}_m\theta_m(m=1,2,3\ldots M) \tag{7}$$

Subject to

$$-\bar{k}_1\frac{\partial\theta_1}{\partial\xi}+\bar{k}_1\frac{Pe_1}{\bar{\alpha}_1}\theta_1+Bi_A\theta_1=0 \ at \ \xi=0 \tag{8}$$

$$\bar{k}_M\frac{\partial\theta_M}{\partial\xi}-\bar{k}_M\frac{Pe_M}{\bar{\alpha}_M}\theta_M+Bi_B\theta_M=0 \ at \ \xi=1 \tag{9}$$

$$\theta_m=\theta_{m+1} \ at \ \xi=\gamma_m \ (m=1,2\ldots M-1) \tag{10}$$

$$-\bar{k}_m\frac{\partial\theta_m}{\partial\xi}+\bar{k}_m\frac{Pe_m}{\bar{\alpha}_m}\theta_m=-\bar{k}_{m+1}\frac{\partial\theta_{m+1}}{\partial\xi}+\bar{k}_{m+1}\frac{Pe_{m+1}}{\bar{\alpha}_{m+1}}\theta_{m+1} \ at \ \xi=\gamma_m(m=1,2\ldots M-1) \tag{11}$$

$$\theta_m=\theta_{m,0}(\xi) \ at \ \tau=0 \ (m=1,2.,..M) \tag{12}$$

A separable form of the solution, $\theta_m(\xi,\tau)=\sum_{n=1}^{\infty}f_{m,n}(\xi)g_n(\tau)$ (m = 1,2,...*M*) may be assumed in order to solve Eqs. (7)-(12). By substituting the assumed form in Eq. (7), it can be shown that $g_n(\tau)=\exp(-\lambda_n^2\tau)$, where λ_n are the eigenvalues. In addition, the functions $f_{m,n}$ satisfy $\bar{\alpha}_m f''_{m,n}-Pe_m f'_{m,n}+\bar{\beta}_m f_{m,n}=-\lambda_n^2 f_{m,n}$ (m = 1,2...*M*). A general solution for $f_{m,n}$ comprises a product of periodic functions with an exponential function to account for the Pe_m term [17]. A solution for θ_m can, therefore, be written as follows:

$$\theta_m(\xi,\tau)=\sum_{n=1}^{\infty}c_n[A_{m,n}\cos(\omega_{m,n}\xi)+B_{m,n}\sin(\omega_{m,n}\xi)]\exp\left(\frac{Pe_m\xi}{2\bar{\alpha}_m}\right)\exp\left(-\lambda_n^2\tau\right) \tag{13}$$

where $\omega_{m,n}$ are the spatial eigenvalues, which, by substituting Eq. (13) in the governing Eq. (7) can be shown to be given by

$$\omega_{m,n}=\sqrt{\frac{\lambda_n^2+\bar{\beta}_m^*}{\bar{\alpha}_m}}(m=1,2..M) \tag{14}$$

where $\bar{\beta}_m^* = \bar{\beta}_m - Pe_m^2/(4\bar{\alpha}_m)$.

Now, $A_{m,n}$, $B_{m,n}$ and λ_n are to be determined using the boundary and interface conditions given by Eqs. (8)-(11). Inserting Eq. (13) in Eqs. (8)-(11) results in

$$-\bar{k}_1\omega_{1,n}B_{1,n} + Bi_A^* A_{1,n} = 0 \tag{15}$$

$$\bar{k}_M\omega_{M,n}[-A_{M,n}sin(\omega_{M,n}) + B_{M,n}cos(\omega_{M,n})] + Bi_B^*[A_{M,n}cos(\omega_{M,n}) + B_{M,n}sin(\omega_{M,n})] = 0 \tag{16}$$

$$\exp\left(\frac{Pe_m\gamma_m}{2\bar{\alpha}_m}\right)[A_{m,n}cos(\omega_{m,n}\gamma_m) + B_{m,n}sin(\omega_{m,n}\gamma_m)] = \exp\left(\frac{Pe_{m+1}\gamma_m}{2\bar{\alpha}_{m+1}}\right)[A_{m+1,n}cos(\omega_{m+1,n}\gamma_m) + B_{m+1,n}sin(\omega_{m+1,n}\gamma_m)] \tag{17}$$

$$\begin{aligned}&\bar{k}_m\exp\left(\frac{Pe_m\gamma_m}{2\bar{\alpha}_m}\right)\left[\omega_{m,n}(-A_{m,n}sin(\omega_{m,n}\gamma_m) + B_{m,n}cos(\omega_{m,n}\gamma_m)) - \frac{Pe_m}{2\bar{\alpha}_m}(A_{m,n}cos(\omega_{m,n}\gamma_m) + B_{m,n}sin(\omega_{m,n}\gamma_m))\right]\\ &= \bar{k}_{m+1}\exp\left(\frac{Pe_{m+1}\gamma_m}{2\bar{\alpha}_{m+1}}\right)\left[\omega_{m+1,n}(-A_{m+1,n}sin(\omega_{m+1,n}\gamma_m) + B_{m+1,n}cos(\omega_{m+1,n}\gamma_m)) - \frac{Pe_{m+1}}{2\bar{\alpha}_{m+1}}(A_{m+1,n}cos(\omega_{m+1,n}\gamma_m) + B_{m+1,n}sin(\omega_{m+1,n}\gamma_m))\right]\end{aligned} \tag{18}$$

where $Bi_A^* = Bi_A + \frac{\bar{k}_1 Pe_1}{2\bar{\alpha}_1}$ and $Bi_B^* = Bi_B - \frac{\bar{k}_M Pe_M}{2\bar{\alpha}_M}$ may be interpreted as the modified Biot numbers that account for advection at the boundaries. Note that Eqs. (17) and (18) hold for m = 1,2,...M-1.

Eqs. (15)-(18) represent a set of 2 M homogeneous equations in $A_{m,n}$ and $B_{m,n}$ (m = 1,2..M). The eigenvalues λ_n are also unknown, which can be determined by requiring Eqs. (15)-(18) to admit a non-trivial solution. The following procedure systematically eliminates the coefficients from these equations in order to derive an explicit eigenequation for the M–layer case.

From Eqs. (15)-(18), one may write

$$f_{m,n}(\xi) = A_{1,n}\Phi_m p_{m,n}(\xi) \tag{19}$$

Where

$$\Phi_m = \frac{p_{m-1,n}(\gamma_{m-1})}{p_{m,n}(\gamma_{m-1})}\cdot\frac{p_{m-2,n}(\gamma_{m-2})}{p_{m-1,n}(\gamma_{m-2})}\cdots\frac{p_{2,n}(\gamma_2)}{p_{3,n}(\gamma_2)}\cdot\frac{p_{1,n}(\gamma_1)}{p_{2,n}(\gamma_1)} \quad (m = 2, 3, ..M) \tag{20}$$

with

$$p_{m,n}(\xi) = [cos(\omega_{m,n}\xi) + \psi_{m,n}(\lambda_n)sin(\omega_{m,n}\xi)]\exp\left(\frac{Pe_m\xi}{2\bar{\alpha}_m}\right) \tag{21}$$

Note that $\Phi_1 = 1$. Further, the functions $\psi_{m,n}(\lambda_n)$ in Eq. (21) are given by

$$\psi_{1,n}(\lambda_n) = \frac{Bi_A^*}{\bar{k}_1\omega_{1,n}} \tag{22}$$

$$\begin{aligned}&\psi_{m+1,n}(\lambda_n) = \\ &-\left[\bar{k}_m\cos(\omega_{m+1,n}\gamma_m)p'_{m,n}(\gamma_m) - \bar{k}_m\frac{Pe_m}{\bar{\alpha}_m}\cos(\omega_{m+1,n}\gamma_m)p_{m,n}(\gamma_m) - \bar{k}_{m+1}\omega_{m+1,n}\sin(\omega_{m+1,n}\gamma_m)p_{m,n}(\gamma_m) + \bar{k}_{m+1}\frac{Pe_{m+1}}{2\bar{\alpha}_{m+1}}\cos(\omega_{m+1,n}\gamma_m)p_{m,n}(\gamma_m)\right]\Big/\\ &\left[\bar{k}_m\sin(\omega_{m+1,n}\gamma_m)p'_{m,n}(\gamma_m) - \bar{k}_m\frac{Pe_m}{\bar{\alpha}_m}\sin(\omega_{m+1,n}\gamma_m)p_{m,n}(\gamma_m) - \bar{k}_{m+1}\omega_{m+1,n}\cos(\omega_{m+1,n}\gamma_m)p_{m,n}(\gamma_m) + \bar{k}_{m+1}\frac{Pe_{m+1}}{2\bar{\alpha}_{m+1}}\sin(\omega_{m+1,n}\gamma_m)p_{m,n}(\gamma_m)\right]\\ &(m = 1, 2..M-1)\end{aligned} \tag{23}$$

$$\psi_{M,n}(\lambda_n) = \frac{\left[\bar{k}_M\omega_{M,n}sin(\omega_{M,n}) - Bi_B^*cos(\omega_{M,n})\right]}{\left[\bar{k}_M\omega_{M,n}cos(\omega_{M,n}) + Bi_B^*sin(\omega_{M,n})\right]} \tag{24}$$

The function $\psi_{M,n}(\lambda_n)$ for the M^{th} layer can be obtained from either Eq. (23) by setting m = M-1, or directly from Eq. (24). Therefore, the eigenvalues λ_n can be determined by comparing Eq. (24) with Eq. (23) for m = M-1. This results in

$$\begin{aligned}&\left[\bar{k}_M\omega_{M,n}sin(\omega_{M,n}) - Bi_B^*cos(\omega_{M,n})\right]\Big/\left[\bar{k}_M\omega_{M,n}cos(\omega_{M,n}) + Bi_B^*sin(\omega_{M,n})\right]\\ &+\left[\bar{k}_{M-1}cos(\omega_{M,n}\gamma_{M-1})p'_{M-1,n}(\gamma_{M-1}) - \bar{k}_{M-1}\frac{Pe_{M-1}}{\bar{\alpha}_{M-1}}cos(\omega_{M,n}\gamma_{M-1})p_{M-1,n}(\gamma_{M-1}) - \bar{k}_M\omega_{M,n}sin(\omega_{M,n}\gamma_{M-1})p_{M-1,n}(\gamma_{M-1}) + \bar{k}_M\frac{Pe_M}{2\bar{\alpha}_M}cos(\omega_{M,n}\gamma_{M-1})p_{M-1,n}(\gamma_{M-1})\right]\Big/\\ &\left[\bar{k}_{M-1}sin(\omega_{M,n}\gamma_{M-1})p'_{M-1,n}(\gamma_{M-1}) - \bar{k}_{M-1}\frac{Pe_{M-1}}{\bar{\alpha}_{M-1}}sin(\omega_{M,n}\gamma_{M-1})p_{M-1,n}(\gamma_{M-1}) - \bar{k}_M\omega_{M,n}cos(\omega_{M,n}\gamma_{M-1})p_{M-1,n}(\gamma_{M-1}) + \bar{k}_M\frac{Pe_M}{2\bar{\alpha}_M}sin(\omega_{M,n}\gamma_{M-1})p_{M-1,n}(\gamma_{M-1})\right] = 0\end{aligned} \tag{25}$$

where $\omega_{M,n}$ is given by Eq. (14) for $m = M$.

Eq. (25) represents a transcendental equation in the eigenvalues λ_n. Once the eigenvalues are obtained by determining the roots of Eq. (25), the coefficients $A_{m,n}$ and $B_{m,n}$ can be determined from Eqs. (15)-(17) by assuming, without loss of generality, that $A_{1,n}$ = 1. The principle of orthogonality for this problem is derived in Appendix A, using which, the coefficient c_n appearing in Eq. (13) may be obtained from the initial condition as follows:

$$c_n = \frac{1}{N_n}\left[\sum_{m=1}^{M}\frac{\bar{k}_m}{\bar{\alpha}_m s_m}\int_{\gamma_{m-1}}^{\gamma_m}\theta_{m,0}(\xi)f_{m,n}\exp\left(\frac{-Pe_m\xi}{\bar{\alpha}_m}\right)d\xi\right] \tag{26}$$

where the norm N_n is given by

$$N_n = \left[\sum_{m=1}^{M}\frac{\bar{k}_m}{\bar{\alpha}_m s_m}\int_{\gamma_{m-1}}^{\gamma_m}[f_{m,n}(\xi)]^2\exp\left(\frac{-Pe_m\xi}{\bar{\alpha}_m}\right)d\xi\right] \tag{27}$$

where the coefficients s_m are given by equation (A.5) in Appendix A.

Note that the orthogonality relationship and norm given by equations (A.7) and (27) differ from the standard diffusion-only multilayer problem [1] because of the exponential terms that account for advection, as well as the s_m term that occurs in the general CDR problem.

The special case of a two-layer body is discussed in detail in the next section.

3. Special case: two-layer body

This section considers the special case of the CDR equations for a two-layer body, which is particularly relevant for several engineering applications. Analysis of the two-layer body also reduces the number of parameters, and makes it easier to understand the interplay between diffusion, advection, heat generation and heat removal from the boundaries.

In this case, a solution for temperature fields in the two layers, θ_1 and θ_2 can be written as follows:

$$\theta_1(\xi,\tau) = \sum_{n=1}^{\infty} c_n[A_{1,n}\cos(\omega_{1,n}\xi) + B_{1,n}\sin(\omega_{1,n}\xi)] \exp\left(\frac{Pe_1\xi}{2\bar{\alpha}_1}\right)\exp\left(-\lambda_n^2\tau\right) \tag{28}$$

and

$$\theta_2(\xi,\tau) = \sum_{n=1}^{\infty} c_n[A_{2,n}\cos(\omega_{2,n}\xi) + B_{2,n}\sin(\omega_{2,n}\xi)] \exp\left(\frac{Pe_2\xi}{2\bar{\alpha}_2}\right)\exp\left(-\lambda_n^2\tau\right) \tag{29}$$

where $\omega_{m,n}$ is given by Eq. (14) for $m = 1,2$.

The eigenequation for the two-layer problem can be obtained either by simply putting $M = 2$ in the general M-layer eigenequation given by Eq. (25), or by setting to zero the determinant of the system of equations obtained by inserting Eqs. (28) and (29) in the boundary and interface conditions. The resulting eigenequation is

$$\bar{k}_1\omega_{1,n}\frac{\left[-\bar{k}_1\omega_{1,n} + Bi_A^* cot(\omega_{1,n}\gamma_1)\right]}{\left[\bar{k}_1\omega_{1,n}cot(\omega_{1,n}\gamma_1) + Bi_A^*\right]} - \frac{\bar{k}_1 Pe_1}{2\bar{\alpha}_1} + \bar{k}_2\omega_{2,n}\frac{\left[-\bar{k}_2\omega_{2,n} + Bi_B^* cot(\omega_{2,n}(1-\gamma_1))\right]}{\left[\bar{k}_2\omega_{2,n}cot(\omega_{2,n}(1-\gamma_1)) + Bi_B^*\right]} + \frac{\bar{k}_2 Pe_2}{2\bar{\alpha}_2} = 0 \tag{30}$$

Note that by setting $Pe_1 = Pe_2 = 0$, Eq. (30) reduces to the identical eigenequation that was derived in a recent work for diffusion-reaction problem with no advection [35].

In order to complete the solution for the two-layer case, the coefficients $A_{1,n}$, $B_{1,n}$, $A_{2,n}$ and $B_{2,n}$ may be determined from the boundary and interface conditions, given by

$$-\bar{k}_1\omega_{1,n}B_{1,n} + Bi_A^* A_{1,n} = 0 \tag{31}$$

$$\bar{k}_2\omega_{2,n}[-A_{2,n}sin(\omega_{2,n}) + B_{2,n}cos(\omega_{2,n})] + Bi_B^*[A_{2,n}cos(\omega_{2,n}) + B_{2,n}sin(\omega_{2,n})] = 0 \tag{32}$$

$$\exp\left(\frac{Pe_1\gamma_1}{2\bar{\alpha}_1}\right)[A_{1,n}cos(\omega_{1,n}\gamma_1) + B_{1,n}sin(\omega_{1,n}\gamma_1)] = \exp\left(\frac{Pe_2\gamma_1}{2\bar{\alpha}_2}\right)[A_{2,n}cos(\omega_{2,n}\gamma_1) + B_{2,n}sin(\omega_{2,n}\gamma_1)] \tag{33}$$

$$\bar{k}_1\exp\left(\frac{Pe_1\gamma_1}{2\bar{\alpha}_1}\right)\left[\omega_{1,n}(-A_{1,n}sin(\omega_{1,n}\gamma_1) + B_{1,n}cos(\omega_{1,n}\gamma_1)) - \frac{Pe_1}{2\bar{\alpha}_1}(A_{1,n}cos(\omega_{1,n}\gamma_1) + B_{1,n}sin(\omega_{1,n}\gamma_1))\right] = \bar{k}_2\exp\left(\frac{Pe_2\gamma_1}{2\bar{\alpha}_2}\right)\left[\omega_{2,n}(-A_{2,n}sin(\omega_{2,n}\gamma_1) + B_{2,n}cos(\omega_{2,n}\gamma_1)) - \frac{Pe_2}{2\bar{\alpha}_2}(A_{2,n}cos(\omega_{2,n}\gamma_1) + B_{2,n}sin(\omega_{2,n}\gamma_1))\right] \tag{34}$$

Specifically, since Eqs. (31)-(34) are not linearly independent, one may set $A_{1,n} = 1$ and determine the remaining coefficients from the equations. Finally, using the statement of orthogonality derived in Appendix A for $M = 2$, the coefficient c_n appearing in Eqs. (28)-(29) can be written as

$$c_n = \frac{1}{N_n}\left[\frac{\bar{k}_1}{\bar{\alpha}_1 s_1}\int_0^{\gamma_1}\theta_{1,0}(\xi)f_{1,n}(\xi)\exp\left(\frac{-Pe_1\xi}{\bar{\alpha}_1}\right)d\xi + \frac{\bar{k}_2}{\bar{\alpha}_2 s_2}\int_{\gamma_1}^{1}\theta_{2,0}(\xi)f_{2,n}(\xi)\exp\left(\frac{-Pe_2\xi}{\bar{\alpha}_2}\right)d\xi\right] \tag{35}$$

where the norm N_n is given by

$$N_n = \frac{\bar{k}_1}{\bar{\alpha}_1 s_1}\int_0^{\gamma_1}[f_{1,n}(\xi)]^2\exp\left(\frac{-Pe_1\xi}{\bar{\alpha}_1}\right)d\xi + \frac{\bar{k}_2}{\bar{\alpha}_2 s_2}\int_{\gamma_1}^{1}[f_{2,n}(\xi)]^2\exp\left(\frac{-Pe_2\xi}{\bar{\alpha}_2}\right)d\xi \tag{36}$$

This completes the solution for the special case of the two-layer body. The nature of eigenvalues for this problem is discussed in detail in the next section.

4. Eigenvalue analysis

This section presents an analysis of the eigenvalues for the two-layer case described in Section 3. Determining the conditions that result in imaginary eigenvalues is of particular interest from both theoretical and practical perspectives, since an imaginary value of λ_n will cause exponential rise in temperature at large times, which corresponds to thermal runaway. Therefore, in order to ensure safety and reliability of engineering systems modeled by these equations, it is critical to understand the conditions in which imaginary eigenvalues occur.

Two types of imaginary eigenvalues may appear in this problem. Firstly, in order to determine if Eqn. 30 may admit any imaginary roots, one may substitute $\hat{\lambda}_n = i\cdot\lambda_n$, where $i = \sqrt{-1}$ is the unit imaginary number. By doing so, the eigenequation may be rewritten as

$$f(\hat{\lambda}) = \bar{k}_1\hat{\omega}_{1,n}\frac{\left[\bar{k}_1\hat{\omega}_{1,n} + Bi_A^* coth(\hat{\omega}_{1,n}\gamma_1)\right]}{\left[\bar{k}_1\hat{\omega}_{1,n}coth(\hat{\omega}_{1,n}\gamma_1) + Bi_A^*\right]} - \frac{\bar{k}_1 Pe_1}{2\bar{\alpha}_1} + \bar{k}_2\hat{\omega}_{2,n}\frac{\left[\bar{k}_2\hat{\omega}_{2,n} + Bi_B^* coth(\hat{\omega}_{2,n}(1-\gamma_1))\right]}{\left[\bar{k}_2\hat{\omega}_{2,n}coth(\hat{\omega}_{2,n}(1-\gamma_1)) + Bi_B^*\right]} + \frac{\bar{k}_2 Pe_2}{2\bar{\alpha}_2} = 0 \tag{37}$$

where $\hat{\omega}_{m,n} = \sqrt{\frac{\hat{\lambda}_n^2 - \bar{\beta}_m^*}{\bar{\alpha}_m}} = i\cdot\omega_{m,n}$ for $m = 1,2$

Now, $f(\hat{\lambda}_n)$ is an increasing function for positive values of $\hat{\lambda}_n$ [35], and therefore, in order for a root of Eq. (37) to exist, corresponding to an imaginary eigenvalue, it is necessary and sufficient that the value of the function $f(\hat{\lambda}_n)$ be negative at $\hat{\lambda}_n = 0$. Therefore, a limiting condition for an imaginary eigenvalue to exist for the two-layer CDR problem is that

$$f(0) = \bar{k}_1\frac{\left[-\bar{k}_1\bar{\beta}_1^*/\bar{\alpha}_1 + Bi_A^*\sqrt{\bar{\beta}_1^*/\bar{\alpha}_1}cot\left(\sqrt{\bar{\beta}_1^*/\bar{\alpha}_1}\gamma_1\right)\right]}{\left[\bar{k}_1\sqrt{\bar{\beta}_1^*/\bar{\alpha}_1}cot\left(\sqrt{\bar{\beta}_1^*/\bar{\alpha}_1}\gamma_1\right) + Bi_A^*\right]} - \frac{\bar{k}_1 Pe_1}{2\bar{\alpha}_1} + \bar{k}_2\frac{\left[-\bar{k}_2\bar{\beta}_2^*/\bar{\alpha}_2 + Bi_B^*\sqrt{\frac{\bar{\beta}_2^*}{\bar{\alpha}_2}}cot\left(\sqrt{\frac{\bar{\beta}_2^*}{\bar{\alpha}_2}}(1-\gamma_1)\right)\right]}{\left[\bar{k}_2\sqrt{\frac{\bar{\beta}_2^*}{\bar{\alpha}_2}}cot\left(\sqrt{\frac{\bar{\beta}_2^*}{\bar{\alpha}_2}}(1-\gamma_1)\right) + Bi_B^*\right]} + \frac{\bar{k}_2 Pe_2}{2\bar{\alpha}_2} < 0 \tag{38}$$

Due to the monotonically increasing nature of $f(\hat{\lambda})$, at most one imaginary eigenvalue may be expected.

A special case of Eq. (38) can be considered where the boundary conditions are isothermal. This can be modeled by setting the Biot numbers to infinity, which results in the following limiting condition for an imaginary eigenvalue to exist for the isothermal problem

$$\bar{k}_1\sqrt{\bar{\beta}_1^*/\bar{\alpha}_1}cot\left(\sqrt{\bar{\beta}_1^*/\bar{\alpha}_1}\gamma_1\right) - \frac{\bar{k}_1 Pe_1}{2\bar{\alpha}_1} + \bar{k}_2\sqrt{\frac{\bar{\beta}_2^*}{\bar{\alpha}_2}}cot\left(\sqrt{\frac{\bar{\beta}_2^*}{\bar{\alpha}_2}}(1-\gamma_1)\right) + \frac{\bar{k}_2 Pe_2}{2\bar{\alpha}_2} < 0 \quad (39)$$

Eq. (39) represents a weaker condition for an imaginary eigenvalue to exist compared to the condition for the general case, because an isothermal boundary condition results in more effective heat removal from the boundaries.

Note that based on Eq. (13), an imaginary value of $\lambda_1$will result in infinite temperature at large time due to the exponential term in the solution. Eq. (38) represents a complex interplay between advection (Pe), generation ($\bar{\beta}$), diffusion ($\bar{\alpha}$) and convective heat removal at the boundaries (Bi) to determine whether an imaginary eigenvalue, and therefore, thermal runaway occurs or not. In general, imaginary eigenvalues may be expected when heat generation dominates over heat removal, i.e., large positive values of $\bar{\beta}_1$ and/or $\bar{\beta}_2$, and small values of Bi_A and/or Bi_B. The role of advection, represented by Pe_1 and Pe_2 may be more complicated to discern, and is discussed in detail in Section 5.

In addition to the eigenequation given by Eq. (38) resulting in an imaginary eigenvalue λ_1, Eq. (14) shows that the spatial eigenvalues $\omega_{m,n}$ may also become imaginary under certain conditions. This is referred to as the second type of imaginary eigenvalues in this work. Specifically, the condition for an imaginary $\omega_{m,n}$ may be written as

$$\lambda_n^2 + \bar{\beta}_m - \frac{Pe_m^2}{4\bar{\alpha}_m} < 0 \quad (40)$$

Eq. (40) shows that an imaginary value of $\omega_{m,n}$ may be expected for large Pe_m, small $\bar{\alpha}_m$, large negative $\bar{\beta}_m$ and for imaginary λ_n, if one exists according to Eq. (38). This condition on $\bar{\beta}_m$ is opposite to the conditions in which the first type of imaginary eigenvalues occur. In addition, if the condition given by Eq. (40) is satisfied, a mix of imaginary and real eigenvalues may be expected. The first few eigenvalues may become imaginary because λ_n is small in magnitude for small n. As λ_n increases in magnitude with increasing n, it is expected that subsequent eigenvalues will be real. Eq. (40) also shows that eigenvalues of one layer may become imaginary while those of other layers may all continue to be real, depending on the values of various parameters in the layers. Note that an imaginary value of $\omega_{m,n}$ does not cause thermal runaway, since $\omega_{m,n}$ does not appear in an exponential term in the temperature solution given by Eqs. (28) and (29). Also note that past work [35] has shown that the temperature distribution remains real even if the eigenvalues appearing in the periodic terms are imaginary.

Since the occurrence of imaginary eigenvalues is of practical importance for predicting thermal runaway, a detailed discussion on the impact of various problem parameters on the appearance of imaginary eigenvalues is presented in the next section.

5. Discussion

Before discussing the impact of various problem parameters on the occurrence of imaginary eigenvalues in the problem, the accuracy of the analysis presented in this work is established. Specifically, the predicted temperature distribution for a two-layer body based on Eq. (28) and (29) is compared against numerical simulations based on the finite-difference method. For this purpose, the governing equation and boundary conditions in each layer are discretized using a second-order central difference formula in space and a fully implicit scheme in time. A node at the interface is defined to apply the required interfacial conditions and ensure continuity. 1000 nodes and 1000 intervals are used for space and time discretization, respectively. The resultant algebraic equations has been solved using a Tridiagonal Matrix Algorithm (TDMA). Two contrasting scenarios are considered for this comparison. In the first scenario, both source coefficients $\bar{\beta}_1$ and $\bar{\beta}_2$ are negative, based on which, temperature distribution is expected to stay bounded as time passes. A comparison of temperature distributions at multiple times predicted by the analytical model and numerical simulations is presented in Fig. 2(a) for an initial temperature of 1 throughout. As expected, due to the negative values of both source coefficients, temperature stays bounded, and there is very good agreement between the analytical model and numerical simulations at each time. On the other hand, a scenario with $\bar{\beta}_1 = 0$ and $\bar{\beta}_2 = 18$ is considered in Fig. 2(b). In this case, the large source coefficient in the second layer dominates over advection and convective heat removal at the boundaries to result in thermal runaway at large times, as shown in Fig. 2(b). The temperature distributions at various times predicted by the analytical model remains in good agreement with numerical simulations, even when there is exponential temperature rise with time.

It is of interest to determine the regimes of various problem parameters in which imaginary eigenvalues may appear in the CDR problem. Thermal diffusivities, Peclet numbers and the source coefficients are the key parameters that represent diffusion, advection and generation, respectively. A complex interplay between these parameters, as represented in Eqs. (38) and (40) ultimately determines whether the problem has imaginary eigenvalues, and whether the temperature field diverges at large times. These considerations are discussed next in the context of a two-layer problem.

Fig. 3 investigates the impact of Peclet numbers on the eigenequation. Specifically, the eigenequation, Eq. (30) is plotted for three different values of Pe_1 and Pe_2 in Figs. 3(a) and 3(b), respectively in the imaginary regime. Note that an imaginary eigenvalue exists if the eigenequation curve crosses the x axis. These plots show that changing Pe_2 has a much stronger impact on the eigenequation than changing Pe_1. In general, increasing Pe_2 shifts the eigenequation upwards and away from the appearance of an imaginary eigenvalue. On the other hand, increasing Pe_1 shifts the curves slightly downwards. This is consistent with the physical understanding of advection in this problem. Since the flow is assumed to be from left to right in this problem, therefore, advection in the second layer facilitates removal of heat from the body into the ambient. As a result, greater value of Pe_2 will move the eigenequation away from the x axis. On the other hand, Pe_1 advects heat into the body, and therefore, increasing Pe_1 is expected to contribute towards thermal runaway. Both of these considerations are consistent with the results shown in Fig. 3. Fig. 3 is also consistent with Eq. (38), in that Eq. (38) shows that increasing Pe_1 will reduce the value of the eigenfunction f, whereas increasing Pe_2 has the opposite effect.

Note that Fig. 3 is plotted for fixed values of the source coefficients $\bar{\beta}_1$ and $\bar{\beta}_2$. To further investigate this and account for the effect of heat generation, Fig. 4 plots the magnitude of the imaginary eigenvalue as a function of advection for multiple values of the source term. Figs. 4(a) and 4(b) present these plots for parameters related to the first and second layers, respectively. Consistent with Fig. 3, Fig. 4 shows much greater sensitivity of the imaginary eigenvalue on Pe_2 than Pe_1. When the value of Pe_2 exceeds a certain threshold, the imaginary eigenvalue is eliminated com-

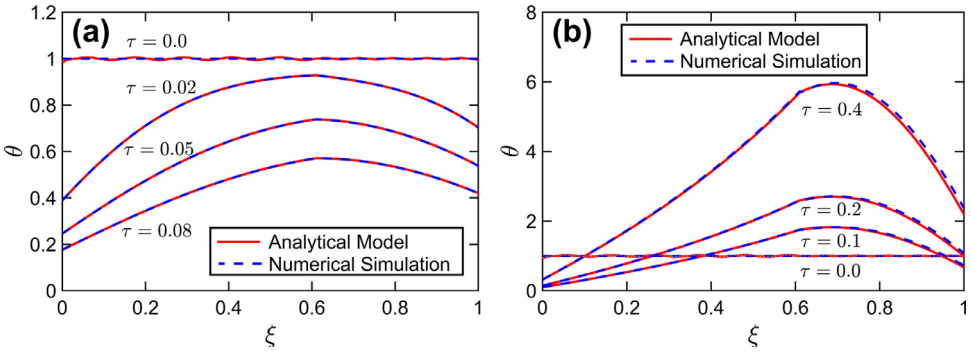

Fig. 2. Comparison of predicted temperature distribution for a two-layer body with numerical simulations: θ vs ξ at multiple values of τ for (a) converging and (b) diverging temperature distributions. For (a), $Bi_A = Bi_B = 2$; $\tilde{\beta}_1 = -3$; $\tilde{\beta}_2 = -5$, and for (b), $Bi_A = Bi_B = 10$; $\tilde{\beta}_1 = 0$; $\tilde{\beta}_2 = 18$. Other parameters are $\tilde{k}_1 = 0.5$; $\tilde{\alpha}_1 = 2.0$; $Pe_1 = 1$; $Pe_2 = 0.25$; $\gamma_1 = 0.61$.

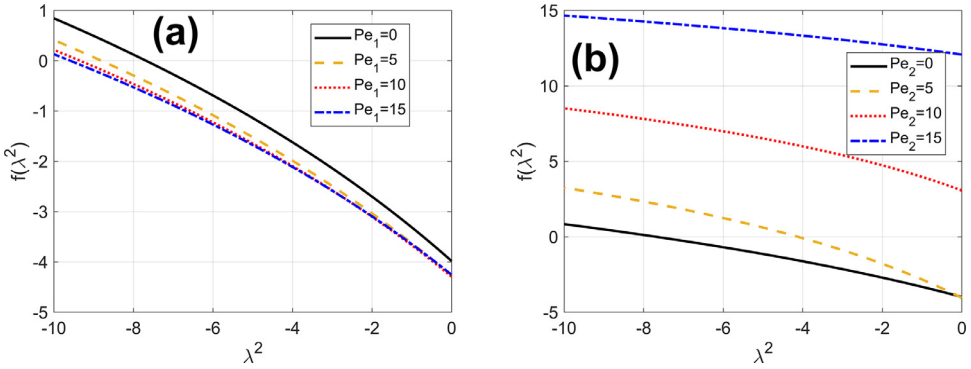

Fig. 3. Plot of the eigenequation for imaginary values of λ: (a) plots the eigenequation for four different values of Pe_1, with $Pe_2 = 0$, and (b) plots the eigenequation for four different values of Pe_2, with $Pe_1 = 0$. Other parameters are $\tilde{k}_1 = 0.5$; $\tilde{\alpha}_1 = 2.0$; $Bi_A = Bi_B = 2$; $\tilde{\beta}_1 = 5$; $\tilde{\beta}_2 = 15$; $\gamma_1 = 0.667$.

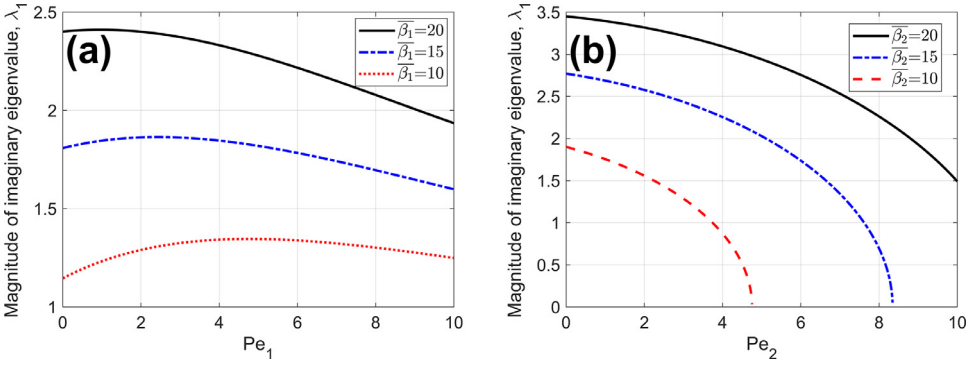

Fig. 4. Plot of the magnitude of the imaginary eigenvalue as a function of (a) Pe_1 for three different values of $\tilde{\beta}_1$with $Pe_2 = 0$ and $\tilde{\beta}_2 = 5$; (b) Pe_2 for three different values of $\tilde{\beta}_2$with $Pe_1 = 0$ and $\tilde{\beta}_1 = 5$. Other parameters are $\tilde{k}_1 = 0.5$; $\tilde{\alpha}_1 = 2.0$; $Bi_A = Bi_B = 2$; $\gamma_1 = 0.667$.

pletely. In this regime, the effect of advection in removing heat from the body is enough to overcome generation, and therefore, thermal runaway does not occur at all. The curves in Fig. 4(b) shift upwards as $\tilde{\beta}_2$ increases, which is because at a greater rate of heat generation, a greater amount of advection is needed to keep the temperature bounded. Compared to the plots in Fig. 4(b), the sensitivity on Pe_1 is not as strong, as shown in Fig. 4(a). While there is a monotonic reduction in λ_1 with Pe_2, λ_1 actually increases slightly and then decreases as Pe_1 increases. In the range of Pe_1 shown in Fig. 4(a), no value is found to avoid thermal runaway, unlike Pe_2, which has a threshold value as shown in Fig. 4(b).

The interplay between advection and generation is expected to occur in practical engineering systems such as a flow battery, and is critical in determining whether thermal runaway occurs or not. Fig. 5 investigates this by identifying regions in the Pe-$\tilde{\beta}$ space corresponding to real and imaginary eigenvalues according to Eq. (28). These colorplots are presented for the first and second layer in Figs. 5(a) and 5(b), respectively. In both cases, small $\tilde{\beta}$ and large Pe results in real eigenvalues, whereas the imaginary eigenvalue occurs when generation is large and advection is small. This is expected because thermal runaway occurs due to an imbalance between heat generation and removal, i.e., when too much heat is generated and too little is removed. As expected, there is no imaginary eigenvalue of the first type if both $\tilde{\beta}_1$ and $\tilde{\beta}_2$ are zero or negative.

Convective boundary conditions at the two ends of the body, represented by Bi_A and Bi_B also play a key role in determining whether thermal runaway occurs or not. While Figs. 3, 4 and 5 are plotted for a fixed value of the Biot numbers, the impact of Biot number on imaginary eigenvalues is investigated next. Fig. 6 plots the minimum value of Pe_2 needed to avoid thermal runaway as a function of Bi for three different values of the source coefficient $\tilde{\beta}_2$.

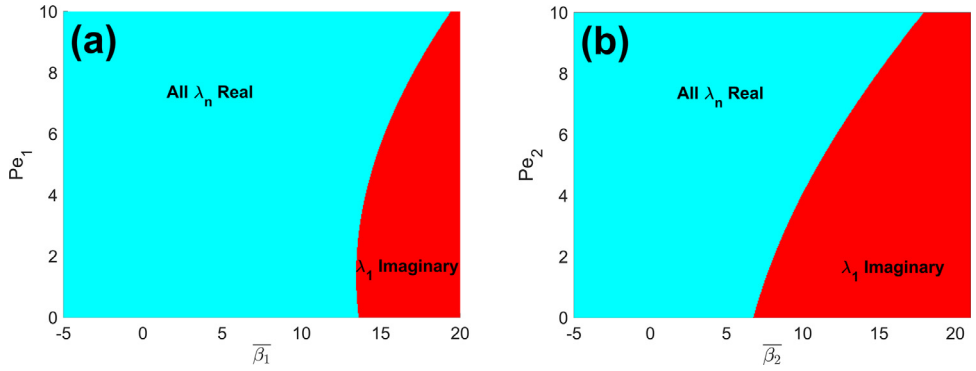

Fig. 5. Colormap showing regimes in the advection-generation spaces for (a) Layer 1, and (b) Layer 2 of a two-layer body, indicating the regions where one of the eigenvalues λ is imaginary. In (a), $Pe_2 = 0$ and $\bar{\beta}_2 = 0$, while in (b), $Pe_1 = 0$ and $\bar{\beta}_1 = 0$. Other parameters are $\bar{k}_1 = 0.5; \bar{\alpha}_1 = 2.0; Bi_A = Bi_B = 2;\ \gamma_1 = 0.667$.

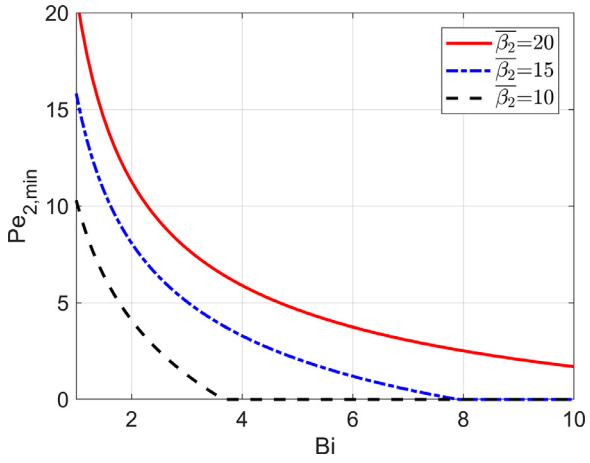

Fig. 6. Plot of the minimum Pe_2 needed to avoid divergence as a function of Bi for a two-layer problem. Plots are shown for three different values of $\bar{\beta}_2$. Other parameter values are $\bar{k}_1 = 0.5; \bar{\alpha}_1 = 2.0; \bar{\beta}_1 = 0; Pe_1 = 0;\ \gamma_1 = 0.667$.

The same Biot number is assumed on both boundaries, and there is no generation in the first layer, as may be the case in several realistic two-layer problems where one of the layers is passive in nature. Fig. 6 shows that, for a given $\bar{\beta}_2$, the minimum Pe_2 needed to avoid thermal runaway reduces with increasing Bi. This is expected because both advection and the convective boundary condition help keep the temperature distribution bounded. Therefore, the greater the value of Bi, corresponding to more effective convective cooling at the boundary, the lower is the value of Pe_2 needed to avoid thermal runaway. Fig. 6 shows that the curve for minimum Pe_2 shifts upwards as $\bar{\beta}_2$ increases, which is also consistent with the expectation that greater heat generation will require greater advection for avoiding thermal runaway through heat removal. Note that for any given $\bar{\beta}_2$, there is a maximum Bi, beyond which, the convective boundary condition is strong enough to avoid thermal runaway by itself even if there is no advection at all. This is the reason why the curves shown in Fig. 6 are expected to flatten out at a threshold Bi value.

In addition to the first eigenvalue λ_1 turning imaginary due to relatively large source coefficients, low advection and/or insufficient heat removal from the boundaries, the CDR problem discussed here may also result in imaginary values of $\omega_{m,n}$. As discussed in Section 4, $\omega_{1,n}$ may become imaginary if Pe_1 is large, $\bar{\alpha}_1$ is negative and/or $\bar{\beta}_1$ is small, and similarly for the eigenvalues of the second layer, $\omega_{2,n}$. Fig. 7 presents a colorplot of the Pe_1-$\bar{\beta}_1$ space, showing the regions where the first spatial eigenvalue of the first layer, $\omega_{1,1}$ turns imaginary. As expected, this occurs for large values of Pe_1, and relatively small values of $\bar{\beta}_1$. A similar plot for the second layer shows quantitative differences between the two layers. In this case, imaginary eigenvalues are expected for large Pe_2, even when $\bar{\beta}_2$ may be somewhat large. This asymmetry between the two layers is due to the differences in the thermal diffusivities. In this case, $\bar{\alpha}_1 = 0.5$, i.e., the first layer has lower diffusivity than the second layer, which results in greater sensitivity of the occurrence of imaginary eigenvalues on $\bar{\beta}_1$ compared to the second layer since thermal diffusivity appears in the denominator of Eq. (40). Note that Fig. 7 is plotted for fixed values of Bi_A and Bi_B that represent the convective boundary conditions.

Also, note that imaginary values of $\omega_{m,n}$ do not impact boundedness of the temperature distribution at large times, unlike the imaginary temporal eigenvalue λ_1. This is because while λ_1 appears in the exponential term in Eq. (13) that may diverge at large times for imaginary value of λ_1, on the other hand, $\omega_{m,n}$ appear only in spatial terms within periodic functions that do not diverge even for imaginary eigenvalues. Note that a recent paper has shown that the temperature distribution for a problem comprising diffusion and generation remains real even if some of the eigenvalues may be imaginary [35]. This was proved in a recursive fashion on the basis of the form of the temperature distribution. Since the temperature distribution for the present problem that also includes advection given by Eq. (13) is similar to the past work, the same result also holds for the present work. This is physically quite reasonable because an imaginary eigenvalue is a mathematical phenomenon, despite which, the temperature distribution for a physically well-defined problem must be expected to be real.

Finally, thermal analysis of a practical application of a two-layer CDR problem is carried out. In the context of a two-layer flow battery, it is important to understand the limits in which thermal runaway of the battery will be avoided when heat is generated due to temperature-dependent decomposition reactions. Note that decomposition reactions for different battery chemistries have different temperature-dependent heat generation characteristics, i.e., values of $\bar{\beta}$. For a given set of external cooling conditions, i.e. given Bi on both ends, calculations are carried out to determine the maximum value of $\bar{\beta}_2$ in which the temperature field will still remain bounded. This analysis is carried out non-dimensionally in order to retain generality of the results, since the geometry and other properties of batteries vary significantly. In this case, a constant value of 0.5 is assumed for the source coefficient in the first layer, $\bar{\beta}_1$. Results are plotted in Fig. 8 for five different values of Pe, which is assumed to be the same in both layers, as may be the case in a practical flow battery. Fig. 8 shows that the greater the value of Pe, the greater is the maximum value of $\bar{\beta}_2$ before thermal runaway occurs. This is along expected lines because advection causes removal of heat from the second layer, which, in this case, has greater heat

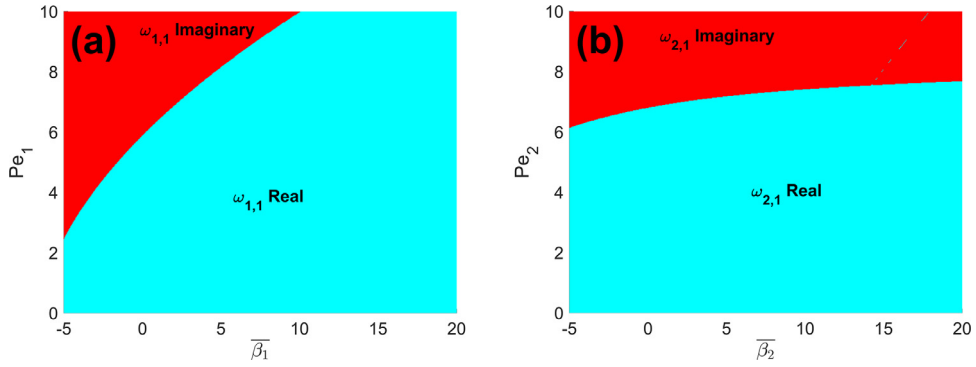

Fig. 7. Colormap showing regimes in the advection-generation spaces for (a) Layer 1, and (b) Layer 2 of a two-layer body, indicating the regions where the first spatial eigenvalue is imaginary. In (a), $Pe_2 = 0$ and $\tilde{\beta}_2 = 0$, while in (b), $Pe_1 = 0$ and $\tilde{\beta}_1 = 0$. Other parameters are $\tilde{k}_1 = 0.5; \tilde{\alpha}_1 = 2.0; Bi_A = Bi_B = 2;\ \gamma_1 = 0.667$.

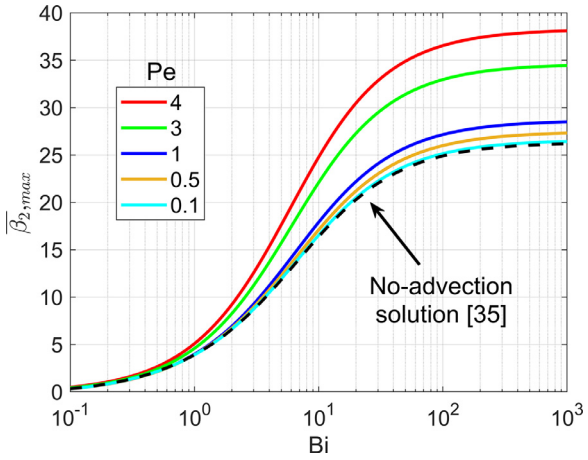

Fig. 8. Practical application of the theoretical model: Plot of the maximum value of $\tilde{\beta}_2$ as a function of *Bi* in order to avoid thermal runaway in a two-layer flow battery. Plots for different values of $Pe_1 = Pe_2 = Pe$ are presented. Other parameters are $\tilde{k}_1 = 0.5; \tilde{\alpha}_1 = 2.0; \tilde{\beta}_1 = 0.5; \gamma_1 = 0.667$.

generation than the first layer. Fig. 8 also shows that for a given *Pe*, the maximum value of $\tilde{\beta}_2$ before thermal runaway first increases slowly as external cooling conditions improve, i.e., as *Bi* increases. This is followed by a region of rapid increase in $\tilde{\beta}_2$ with *Bi*. This effect eventually saturates, as the external cooling approaches the isothermal limit when *Bi* is very large. The greater the value of *Pe*, the large is the isothermal value of $\tilde{\beta}_2$ corresponding to large *Bi*. Finally, it is interesting to note that as *Pe* decreases, the curves in Fig. 8 approach the no-advection curve obtained independently from a past work [35] which analyzed a diffusion-reaction problem with zero advection. This is along expected lines, since *Pe*=0 eliminates advection in the general CDR problem, and reduces it to a diffusion-reaction problem considered in the past paper [35].

6. Conclusions

Theoretical modeling of multilayer CDR problems is important from both theoretical and practical perspectives. The occurrence of imaginary eigenvalues in such problems, even for a one-dimensional geometry, determines whether thermal runaway is encountered or not. In addition, the prediction of conditions in which imaginary eigenvalues appear is important because standard algorithms for computing eigenvalues only focus on real eigenvalues and may miss an imaginary eigenvalue. The analytical solution derived here is for a general *M*-layer body, and can be adapted for other heat/mass transfer scenarios, such as in a porous medium, where the nature of boundary conditions may be different from the ones considered here. Compared to the standard diffusion-only problem, the orthogonality of eigenfunctions for the general multilayer CDR problem derived in this work comprises additional exponential terms that account for advection. On the other hand, the orthogonality remains unaffected by the reaction term. The present work may be considered to be a generalization of recent work [35] in which the effect of advection was not considered. The present work finds that modeling advection results in significant changes in the solutions, particularly, the orthogonality expression and eigenequation is significantly more complicated than in the previous work. While presented in the context of temperature, results from the present work are equally applicable for concentration problems.

Further generalization of the present work to 2D/3D geometries may be of interest. As shown in past work on thermal conduction in a multi-dimensional multi-layer body [31], the direction(s) orthogonal to the layers contribute an additional set of eigenvalues, which themselves may induce imaginary eigenvalues in the normal direction. When coupled with the imaginary eigenvalues shown in this work to occur due to convection and reaction terms, this is likely to make the eigenvalue analysis of the problem even more complicated.

In addition to improving the theoretical understanding of convection-diffusion-reaction problems in a multilayer body, this work may also help understand and optimize heat/mass transfer in practical engineering systems such as flow batteries where a careful balance between heat generation, diffusion, advection and external cooling determines whether thermal runaway may occur.

Declaration of Competing Interest

The authors declare that they have no known competing financial interests or personal relationships that could have appeared to influence the work reported in this paper.

Acknowledgments

This material is based upon work supported by CAREER Award No. CBET-1554183 from the National Science Foundation.

Appendix A. Orthogonality Relationship for *M*-layer Problem

As shown in Section 2, for the m^{th} layer, and for two numbers n and j, the functions $f_{m,n}$ and $f_{m,j}$ satisfy

$$\tilde{\alpha}_m f''_{m,n} - Pe_m f'_{m,n} + \tilde{\beta}_m f_{m,n} = -\lambda_n^2 f_{m,n} \tag{A.1}$$

$$\tilde{\alpha}_m f''_{m,j} - Pe_m f'_{m,j} + \tilde{\beta}_m f_{m,j} = -\lambda_j^2 f_{m,j} \tag{A.2}$$

By multiplying equations (A.1) and (A.2) by $f_{m,j}\exp(\frac{-Pe_m\xi}{\bar{\alpha}_m})$ and $f_{m,n}\exp(\frac{-Pe_m\xi}{\bar{\alpha}_m})$, respectively, and then subtracting, one may obtain

$$\left[\bar{\alpha}_m\left(f''_{m,n}f_{m,j}-f''_{m,j}f_{m,n}\right)-Pe_m\left(f'_{m,n}f_{m,j}-f'_{m,j}f_{m,n}\right)\right]\exp\left(\frac{-Pe_m\xi}{\bar{\alpha}_m}\right)=-\left(\lambda_n^2-\lambda_j^2\right)f_{m,n}f_{m,j}\exp\left(\frac{-Pe_m\xi}{\bar{\alpha}_m}\right) \quad (A.3)$$

Note that the $\bar{\beta}_m$ term cancels out. Equation (A.3) can be simplified to

$$\bar{\alpha}_m\left[\left(f'_{m,n}f_{m,j}-f'_{m,j}f_{m,n}\right)\exp\left(\frac{-Pe_m\xi}{\bar{\alpha}_m}\right)\right]'=-\left(\lambda_n^2-\lambda_j^2\right)f_{m,n}f_{m,j}\exp\left(\frac{-Pe_m\xi}{\bar{\alpha}_m}\right) \quad (A.4)$$

For m = 1,2,..M, equation (A.4) provides one equation per layer. The equation for each layer is multiplied by $\frac{\bar{k}_m}{\bar{\alpha}_m s_m}$, where s_m are given by the recursive relationship

$$s_{m+1}=s_m\frac{\exp\left(\frac{-Pe_{m+1}\gamma_m}{\bar{\alpha}_{m+1}}\right)}{\exp\left(\frac{-Pe_m\gamma_m}{\bar{\alpha}_m}\right)} \quad (A.5)$$

for m = 1,2..M-1, and $s_1=\exp(\frac{-Pe_1\gamma_1}{\bar{\alpha}_1})$.

Each equation is then integrated from $\xi=\gamma_{m-1}$ to $\xi=\gamma_m$ and added, resulting in

$$-\bar{k}_1\frac{\left[f'_{1,n}(0)f_{1,j}(0)-f'_{1,j}(0)f_{1,n}(0)\right]}{\exp\left(\frac{-Pe_1\gamma_1}{\bar{\alpha}_1}\right)}+\bar{k}_M\exp\left(\frac{-Pe_M}{\bar{\alpha}_M}\right)\frac{\left[f'_{M,n}(1)f_{M,j}(1)-f'_{M,j}(1)f_{M,n}(1)\right]}{s_M}+\sum_{m=2}^{M}\frac{\exp\left(\frac{-Pe_{m-1}\gamma_{m-1}}{\bar{\alpha}_{m-1}}\right)}{s_{m-1}}\left[\bar{k}_{m-1}\left(f'_{m-1,n}(\gamma_{m-1})f_{m-1,j}(\gamma_{m-1})-f'_{m-1,j}(\gamma_{m-1})f_{m-1,n}(\gamma_{m-1})\right)-\bar{k}_m\left(f'_{m,n}(\gamma_{m-1})f_{m,j}(\gamma_{m-1})-f'_{m,j}(\gamma_{m-1})f_{m,n}(\gamma_{m-1})\right)\right]=\left(\lambda_n^2-\lambda_j^2\right)\sum_{m=1}^{M}\frac{\bar{k}_m}{\bar{\alpha}_m s_m}\int_{\gamma_{m-1}}^{\gamma_m}f_{m,n}f_{m,j}\exp\left(\frac{-Pe_m\xi}{\bar{\alpha}_m}\right)d\xi \quad (A.6)$$

The first term on the left hand side of equation (A.6) is zero because from the boundary condition at $\xi=0$, one may write $\bar{k}_1 f'_{1,n}(0)=(Bi_A+\bar{k}_1 Pe_1)f_{1,n}(0)$ and $\bar{k}_1 f'_{1,j}(0)=(Bi_A+\bar{k}_1 Pe_1)f_{1,j}(0)$. Similarly, using the boundary condition at $\xi=1$, the second term on the left-hand side of equation (A.6) may be shown to be zero.

Further, each term within square bracket inside the summation on the left hand side can be shown to be zero as follows: From the interface condition at $\xi=\gamma_{m-1}$ given by Eq. (17), $f_{m-1,n}(\gamma_{m-1})=f_{m,n}(\gamma_{m-1})$ and $f_{m-1,j}(\gamma_{m-1})=f_{m,j}(\gamma_{m-1})$, therefore, each term within square bracket inside the summation on the left hand side of equation (A.6) can be rearranged as $f_{m-1,j}(\gamma_{m-1})[\bar{k}_{m-1}f'_{m-1,n}(\gamma_{m-1})-\bar{k}_m f'_{m,n}(\gamma_{m-1})]-f_{m-1,n}(\gamma_{m-1})[\bar{k}_{m-1}f'_{m-1,j}(\gamma_{m-1})-\bar{k}_m f'_{m,j}(\gamma_{m-1})]$. Finally, from the interface condition at $\xi=\gamma_{m-1}$ given by Eq. (18), $\bar{k}_{m-1}f'_{m-1,n}(\gamma_{m-1})-\bar{k}_{m-1}Pe_{m-1}f_{m-1,n}(\gamma_{m-1})=\bar{k}_m f'_{m,n}(\gamma_{m-1})-\bar{k}_m Pe_m f_{m,n}(\gamma_{m-1})$ and $\bar{k}_{m-1}f'_{m-1,j}(\gamma_{m-1})-\bar{k}_{m-1}Pe_{m-1}f_{m-1,j}(\gamma_{m-1})=\bar{k}_m f'_{m,j}(\gamma_{m-1})-\bar{k}_m Pe_m f_{m,j}(\gamma_{m-1})$. Therefore, each term within the summation on the left hand side of equation (A.6) may be further rearranged as $f_{m-1,j}(\gamma_{m-1})[\bar{k}_{m-1}Pe_{m-1}f_{m-1,n}(\gamma_{m-1})-\bar{k}_m Pe_m f_{m-1,n}(\gamma_{m-1})]-f_{m-1,n}(\gamma_{m-1})[\bar{k}_{m-1}Pe_{m-1}f_{m-1,j}(\gamma_{m-1})-\bar{k}_m Pe_m f_{m-1,j}(\gamma_{m-1})]$, which is zero. Therefore, the left hand side of equation (A.6) is zero, and thus, for distinct values of n and j, one may write the following orthogonality relationship

$$\sum_{m=1}^{M}\frac{\bar{k}_m}{\bar{\alpha}_m s_m}\int_{\gamma_{m-1}}^{\gamma_m}f_{m,n}f_{m,j}\exp\left(\frac{-Pe_m\xi}{\bar{\alpha}_m}\right)d\xi=0, for\ n\neq j \quad (A.7)$$

References

[1] M.D. Mikhailov, M.N. Özişik, Unified Analysis and Solutions of Heat and Mass Diffusion, Dover Publications, New York, 1994 ISBN: 0486678768.
[2] S. Mcginty, A decade of modelling drug release from arterial stents, Math. Biosci. 257 (2014) 80–90.
[3] S.M. Becker, Analytic one dimensional transient conduction into a living perfuse/non-perfuse two layer composite system, Heat Mass Transf. 48 (2012) 317–327.
[4] T.P. Fredman, A boundary identification method for an inverse heat conduction problem with an application in ironmaking, Heat Mass Transf. 41 (2004) 95–103.
[5] K. Daryabeigi, Thermal analysis and design optimization of multilayer insulation for reentry aerodynamic heating, J. Spacecraft Rockets 39 (2002) 509–514.
[6] S.M. Becker, H. Herwig, One dimensional transient heat conduction in segmented fin-like geometries with distinct discrete peripheral convection,', Int. J. Therm. Sci. 71 (2013) 348–362.
[7] L. Choobineh, A. Jain, An explicit analytical model for rapid computation of temperature field in a three-dimensional integrated circuit (3D IC), Int. J. Therm. Sci. 87 (2015) 103–109.
[8] H. French, Heat Transfer and Fluid Flow in Nuclear Systems, 1st Ed., Pergamon Press, 1981.
[9] K. Shah, D. Chalise, A. Jain, Experimental and theoretical analysis of a method to predict thermal runaway in Li-ion cells,', J. Power Sources 330 (2016) 167–174.
[10] I. Esho, K. Shah, A. Jain, Measurements and modeling to determine the critical temperature for preventing thermal runaway in Li-ion cells, Appl. Therm. Eng. 145 (2018) 287–294.
[11] R. Spotnitz, J. Franklin, Abuse behavior of high-power, lithium-ion cells,', J. Power Sources 113 (2003) 81–100.
[12] H.H. Pennes, Analysis of tissue and arterial blood temperatures in the resting human forearm, J. Appl. Physiol. 1 (1948) 93–122.
[13] S. Sengupta, T.K. Sengupta, J.K. Puttam, K.S. Vajjala, Global spectral analysis for convection-diffusion-reaction equation in one and two-dimensions: effects of numerical anti-diffusion and dispersion, J. Comput. Phys. 408 (2020) 109310.
[14] Kennedy, C.A., Carpenter, M.H., Additive RungeKutta schemes for convectiondiffusionreaction equations. Applied numerical mathematics, 44(1-2), pp.139–181.
[15] V. Vodicka, Eindimensionale wärmeleitung in geschichteten körpern, Math. Nachr. 14 (1955) 47–55.
[16] C.W. Tittle, Boundary-value problems in composite media: quasi-orthogonal functions, J. Appl. Phys. 36 (1965) 1486–1488.
[17] G. Pontrelli, F. de Monte, Modeling of mass dynamics in arterial drug-eluting stents, J. Porous Media 12 (2009) 19–28.
[18] B. Vick, M.N. Özişik, An exact analysis of low Peclet number heat transfer in laminar flow with axial conduction, Lett. Heat and Mass Transfer 8 (1981) 1–10.
[19] C.-J. Hsu, Theoretical solutions for low-Péclét-number thermal-entry-region heat transfer in laminar flow through concentric annuli,', Int. J. Heat Mass Transfer 13 (1970) 1907–1924.
[20] G. Pontrelli, F. de Monte, Mass diffusion through two-layer porous media: an application to the drug-eluting stent,', Int. J. Heat Mass Transf. 50 (2007) 3658–3669.
[21] G. Pontrelli, F. de Monte, A multi-layer porous wall model for coronary drug-eluting stents,', Int. J. Heat Mass Transf. 53 (2010) 3629–3637.
[22] S. McGinty, S. McKee, R.M. Wadsworth, C. McCormick, Modeling arterial wall drug concentrations following the insertion of a drug-eluting stent, SIAM J. Appl. Math. 73 (2013) 2004–2028.
[23] E.J. Carr, New semi-analytical solutions for advection–dispersion equations in multilayer porous media, Transp. Porous Media 135 (2020) 39–58.
[24] S. McGinty, G. Pontrelli, A general model of coupled drug release and tissue absorption for drug delivery devices, J. Controlled Release 217 (2015) 327–336.
[25] V. Joshi, R.K. Jaiman, A positivity preserving variational method for multi-dimensional convection–diffusion–reaction equation, J. Comput. Phys. 339 (2017) 247–284.
[26] H. Fendoğlu, C. Bozkaya, M. Tezer-Sezgin, DBEM and DRBEM solutions to 2D transient convection-diffusion-reaction type equations, Eng. Anal. Bound. Elem 93 (2018) 124–134.
[27] R.M. Cotta, C.P. Naveira-Cotta, D.C. Knupp, Convective eigenvalue problems for convergence enhancement of eigenfunction expansions in convection–diffusion problems, J. Thermal Sci. Eng. Appl. 10 (2018) 1–12 021009.
[28] J.S.P. Guerrero, L.C.G. Pimentel, T.H. Skaggs, M.Th. van Genuchten, Analytical solution of the advection–diffusion transport equation using a change-of-variable and integral transform technique, Int. J. Heat Mass Transfer 52 (2009) 3297–3304.

[29] R.M. Cotta, D.C. Knupp, J.N.N. Quaresma, K.M. Lisboa, C.P. Naveira-Cotta, J.L.Z. Zotin, H.K. Miyagawa, Integral transform benchmarks of diffusion, convectiondiffusion, and conjugated problems in complex domains, in: A. Runchal (Ed.), 50 Years of CFD in Engineering Sciences, 2020, pp. 719–750, doi:10.1007/978-981-15-2670-1_20.
[30] M. Mohsen, M. Baluch, An analytical solution of the diffusion-convection equation over a finite domain, Appl. Math. Modelling 7 (1983) 285–287.
[31] A. Haji-Sheikh, J.V. Beck, Temperature solution in multi-dimensional multi--layer bodies,', Int. J. Heat Mass Transfer 45 (2002) 1865–1877.
[32] F. de Monte, Unsteady heat conduction in two-dimensional two slab-shaped regions. Exact closed-form solution and results,', Int. J. Heat Mass Transfer 46 (2003) 1455–1469.
[33] H. Salt, Transient heat conduction in a two-dimensional composite slab. II. Physical interpretation of temperatures modes,', Int. J. Heat Mass Transfer 26 (1983) 1617–1623.
[34] M.D. Mikhailov, M.N. Özişik, Transient conduction in a three-dimensional composite slab, Int. J. Heat Mass Transfer 29 (1986) 340–342.
[35] A. Jain, M. Parhizi, L. Zhou, G. Krishnan, Imaginary eigenvalues in multilayer one-dimensional thermal conduction problem with linear temperature-dependent heat generation,', Int. J. Heat Mass Transf. 170 (2021) 1–10 120993.
[36] M. Skyllas-Kazacos, M.H. Chakrabarti, S.A. Hajimolana, F.S. Mjalli, M. Saleem, Progress in flow battery research and development, J. Electrochem. Soc. 158 (2011) R55.